Clays and Clay Minerals, Vol. 48, No. 5, 563–571, 2000.

ION EXCHANGE OF ZEOLITE Na-P_c WITH Pb^{2+}, Zn^{2+}, AND Ni^{2+} IONS

AGGELIKI MOIROU,[1] AIKATERINI VAXEVANIDOU,[1] GEORGIOS E. CHRISTIDIS,[2] AND IOANNIS PASPALIARIS[1]

[1] National Technical University of Athens, Laboratory of Metallurgy, 15780 Zografos, Greece
[2] Technical University of Crete, Department of Mineral Resources Engineering, 73100 Chania, Greece

Abstract—This paper examines the ion-exchange properties of synthetic zeolite Na-P_c, which was produced from perlite-waste fines and has a SiO_2:Al_2O_3 ratio of 4.45:1 and a cation-exchange capacity (CEC) of 3.95 meq g^{-1}. Although equilibrium is attained rapidly for all three metals, exchange is incomplete, with A_c(max) (maximum equilibrium fraction of the metal in the zeolite) being 0.95 for Pb, 0.76 for Zn, and 0.27 for Ni. In both Na → ½Pb and Na → ½Zn exchange, the normalized selectivity coefficient is virtually constant for ${}^{N}A_c$ (normalized equilibrium fraction of the metal in the zeolite) values of ≤0.6, suggesting a pronounced homogeneity of the available exchange sites. The Gibbs standard free energy, ΔG°, of the Na → ½Pb exchange calculated from the normalized selectivity coefficient is −3.11 kJ eq^{-1} and, for the Na → ½Zn exchange, it is 2.75 kJ eq^{-1}.

Examination of the solid exchange products with X-ray diffraction (XRD) revealed a possible decrease in crystallinity of zeolite Pb-P_c as suggested by the significant broadening and disappearance of diffraction lines. This decrease is associated with a reduction of pore opening, as indicated from Fourier-transform infrared analysis (FTIR), which in turn results in a decrease of the amount of zeolitic water. Thermogravimetric-differential thermogravimetric (TG-DTG) analysis showed that water loss occurs in three steps, the relative significance of which depends on the type of exchangeable cation and subsequently on the type of complex formed with the cation and/or the zeolite channels. Zeolite Na-P_c might be utilized in environmental applications, such as the treatment of acid-mine drainage and electroplating effluents.

Key Words—Heavy Metals, Ion Exchange, Perlite, Selectivity, Selectivity Coefficient, Zeolite P_c, Zeolitization.

INTRODUCTION

Zeolite Na-P is a synthetic mineral which is crystallized hydrothermally from sodium aluminosilicate gels (Barrer *et al.,* 1959; Breck, 1974; Barrer, 1982), thermally treated kaolinite, *i.e.,* metakaolinite (Barrer, 1982), and various types of natural glasses in the temperature range of 60–160°C (Aiello *et al.,* 1971; Burriesci *et al.,* 1984; Antonucci *et al.,* 1985; Giordano *et al.,* 1987; Barth-Wirsching *et al.,* 1993; Christidis *et al.,* 1999). The synthetic zeolites produced from natural glasses have variable purity depending on the composition of the starting materials (Breck, 1983). The formation of zeolites from such materials provides the opportunity for upgrading of mineral resources, which are either not exploited or are not utilized in other industrial applications (Burriesci *et al.,* 1984; Giordano *et al.,* 1987), thus enabling the possibility for production of materials with high added value.

The framework of zeolite Na-P is related to the gismondine-group (Fischer, 1963) and more specifically to gobbinsite, which has been observed in basalts in County Antrim, Northern Ireland (Nawaz and Malone, 1982). Na-P is characterized by a disordered (Si, Al) distribution. The structure of Na-P consists of four linked tetrahedra (S4R-type framework) linked to another 4-ring, forming 8-ring channels, which have free aperture sizes of 2.8 × 4.9 and 3.1 × 4.4 Å. (Breck, 1974). The exchangeable cations are located at channel intersections (Breck, 1974). Zeolite Na-P occurs in three polymorphs, a pseudocubic (Na-P_c), a pseudo tetragonal (Na-P_t), and a rare orthorhombic variety. The latter might be a mixture of zeolite-P and a chabazite-like phase. The pseudo-cubic unit cell of Na-P has a = 10.0 Å as compared with the monoclinic unit cell of gismondine a = 10.02; b = 10.62, and c = 9.84 Å with β = 92° 24′. The framework of Na-P_c is flexible and ion exchange frequently converts Na-P_c to the Na-P_t variety (Barrer and Munday, 1971).

The ion-exchange properties of many common synthetic zeolites such as NaX, NaY, and NaA were thoroughly examined in the past, mainly because of their wide utilization in detergents and ammonium exchangers (Sherry and Walton, 1967; Barrer *et al.,* 1968a, 1968b; Gal *et al.,* 1971; Maes and Cremers, 1975; Fletcher and Townsend, 1981, 1982; Wiers *et al.,* 1982; and many others). The use of zeolites in wastewater purification offers the advantage of a highly improved cation-exchange performance relative to natural counterparts. Synthetic zeolites have not been used for environmental application thus far owing to high cost.

The purpose of this contribution is to present new data on the exchange properties of zeolite Na-P_c, produced from perlite fines, with transition elements, which are often present in industrial effluents and which cause environmental problems, and to assess the possibility for utilization of this material as an exchanger in environmental applications.

THEORETICAL CONSIDERATIONS

The binary exchange between a metal cation A and an exchangeable cation B within a homoionic zeolite

in an electrolyte solution is described by the following reaction:

$$z_B A_s^{z_A+} + z_A B_c^{z_B+} \rightleftharpoons z_B A_c^{z_A-} + z_A B_s^{z_B+} \quad (1)$$

where z_A, z_B are the valencies of the cations A and B and the subscripts s and c refer to the solution and the crystal phase (exchanger), respectively. The preference displayed by the zeolites for one of the cations is expressed by the corrected selectivity coefficient, which describes the exchange process qualitatively and it is defined as:

$$K_G = \frac{A_c^{z_B} m_B^{z_A}}{B_c^{z_A} m_A^{z_B}} \Gamma \quad (2)$$

where m_A and m_B are the molalities of the two cations in the solution and Γ represents the solution-phase activity coefficients fraction ($\gamma_B^{z_A}/\gamma_A^{z_B}$).

The corrected selectivity coefficient is used to calculate the rational equilibrium constant K_a, using the following formula (Gaines and Thomas, 1953):

$$\ln K_a = (z_B - z_A) + \int_0^1 \ln K_G \, dA_c. \quad (3)$$

Finally, evaluation of the thermodynamic equilibrium constant leads to the calculation of the Gibbs standard free energy of the exchange according to the following formula:

$$\Delta G^\circ = -\frac{RT}{z_A z_B} \ln K_a \quad (4)$$

where R is the gas constant and T is the temperature in K.

EXPERIMENTAL

Materials and methods

Zeolite Na-P_c was produced from treatment of fine-grained perlite waste, from the Provatas mine, Milos Island, Greece, in a 600-mL inconel autoclave (Parr Instruments). The perlite fines consist of volcanic glass (>90% of the material), quartz, acidic plagioclase, and biotite (Christidis *et al.*, 1999). The perlite fines were heated at 120°C for 2 h, using 1:10 solid:2 N NaOH ratio. The product was filtered under vacuum, washed thoroughly to pH 7, air-dried, and stored in a dessicator.

The mineralogy of the product was examined by X ray diffraction (XRD) using a Siemens D5000 X-ray diffractometer (40 kV and 30 mA, graphite monochromator, CuKα radiation). Additional information about the internal and especially external linkages (pore openings and double rings) was obtained with Fourier-transform infrared spectroscopy (FTIR) (Perkin Elmer 883 FTIR Spectrometer) using KBr discs (Russell, 1987). The amount of 25 mg of air-dried Na-P_c was diluted in 200 mg KBr. The dehydration stages of zeolite Na-P_c were studied with thermogravimetric-differential thermogravimetric analysis (TG-DTG) (Perkin Elmer TGS-2 thermobalance), using a 10°C/min heating rate and nitrogen atmosphere, in the temperature range 50–700°C.

The chemical composition of zeolite Na-P_c was determined by wet methods. The SiO_2 content of the end product was determined with fusion at 1000°C in a platinum crucible, using a mixture of sodium and potassium carbonate and borax as flux and a 10:1 flux: sample ratio. The remaining major elements were determined by acid digestion, using a mixture of concentrated HF, $HClO_4$, and HNO_3. All elements were analyzed by atomic absorption spectrophotometry (AAS) (Perkin Elmer 2100). Loss on ignition (LOI) was determined by weight difference after calcination of the air-dried zeolite at 1000°C. Determination of the cation-exchange capacity (CEC) of the end product was performed by saturation with 1 M ammonium acetate at pH 7 and 25°C, subsequent distillation with a Kjeldahl microsteam apparatus, and titration against sulfuric acid (0.05 N). All reagents used were pro-analysis grade.

Construction of ion-exchange isotherms

The solutions were prepared using chloride salts of Zn and Ni and nitrate for Pb, in the form of Merck standards. The pH value of the solutions before the experiments was adjusted to 4 to avoid possible precipitation of metal hydroxides (Barrer and Townsend, 1976). pH values <3 were avoided because they were found to cause dissolution of the zeolite. To determine optimum conditions for the exchange reaction, a series of preliminary experiments was performed. The optimum time for the equilibrium experiments was determined via the kinetic study of metal adsorption at 25°C, using contact times ranging from 1 min to 10 d for each metal ion. The optimum solution concentration and solid-liquid ratio were evaluated using different amounts of zeolite, which were equilibrated with solutions of concentrations ranging between 10–300 ppm for the contact time determined from the kinetic experiments.

Ion-exchange isotherms for the systems Na → ½Pb, Na → ½Zn, and Na → ½Ni were constructed at 25°C. The equilibrating solutions contained mixtures of the metal chloride (Zn, Ni) with sodium chloride or nitrate (Pb) and sodium nitrate, with different M^{2+}/Na^+ ratios (where M is any metal) and constant total normality, determined by the preliminary experiments. The concentration of the anions present in the solutions (Cl^-, NO_3^-) were the same as the concentration of Na^+ ions to maintain electrical neutrality in the solutions. Accurately known quantities of ~0.1 g of zeolite were equilibrated with 50-mL aliquots of the solutions for sufficient time as determined in kinetic experiments, in duplicate. After equilibration, each sample was filtered in vacuum, washed with distilled H_2O, and al-

https://doi.org/10.1346/CCMN.2000.0480509 Published online by Cambridge University Press

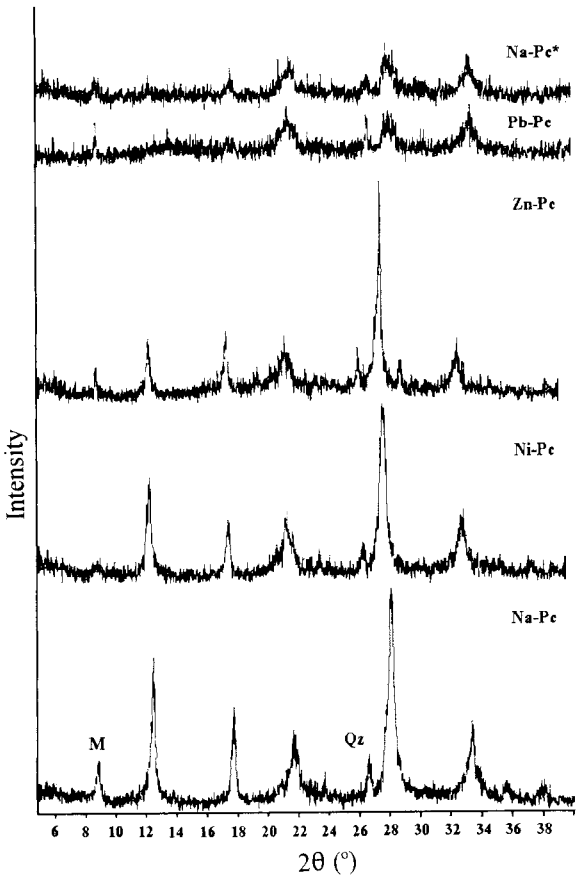

Figure 1. XRD diagrams of the starting zeolite Na-P_c and the solid products of ion exchange. Q = quartz, M = biotite mica. Na-P_c* refers to the zeolite Pb-P_c after being back-exchanged with Na. The broad diffraction hump at a maximum near 14 °2θ is near where the 110 diffraction line should occur prior to "collapse". See text for discussion.

lowed to air-dry. The metal and sodium content of the filtrate was determined by AAS. The pH value of the suspension at equilibrium was <5 in all experiments. Application of the MINTEQA2 (Allison *et al.,* 1991) geochemical modeling software showed that at this pH level it is unlikely that precipitation of metals in the form of hydroxides occurred.

For determination of the reverse isotherm points, weighted amounts of zeolite were equilibrated with metal salt solutions of similar total normality as the forward points for 7 d. The samples were filtered, washed, and air-dried, to avoid dehydration and subsequently possible rearrangement of the exchangeable cations in the zeolite channels. Equilibration with the M^{2+}-saturated zeolite was performed as described for the forward points.

Characterization of the ion-exchange products

The ion-exchange products, zeolites Pb-P_c, Zn-P_c, and Ni-P_c, were examined with XRD and FTIR spectroscopy to determine possible structural modifications and polymorph transitions during ion exchange. The differences in the amount of zeolitic water held by the zeolite P_c when saturated with various metals, compared with the original zeolite Na-P_c, and the response of each material in the various dehydration stages was examined with TG-DTG.

Table 1. Chemical composition of the parent perlite, the end product of zeolitization rich in zeolite Na-P_c, and the pure zeolite Na-P_c. Structural formula (based on 32 O atoms) of the pure zeolite Na-P_c. The molar ratio and the CEC value of pure zeolite Na-P_c in comparison with its theoretical CEC value and the reference value of Barrer and Munday (1971).

	Perlite	Product of zeolitization	Pure zeolite	Structural formula	
SiO_2	72.52	51.29	49.86	Si	10.919
TiO_2	0.10	0.24	n.d.	Al	4.905
Al_2O_3	13.39	19.46	19.02	Fe^{3+}	0.05
Fe_2O_3	1.41	2.21	0.31	Mg^{2+}	0.08
MgO	0.57	0.67	0.19	Ca^{2+}	0.24
CaO	1.15	1.66	0.78	Na	4.43
Na_2O	3.70	10.57	10.44	K	0.35
K_2O	3.41	2.13	1.25		
H_2O	3.21	11.17	17.9	E%	−8.6
Total	99.46	99.34	99.75		

Molar ratio of pure zeolite Na-P_c

$SiO_2:Al_2O_3:(Na_2O + K_2O + CaO + MgO) = 4.45:1:1.06$

CEC of zeolite Na-P_c (meq g^{-1})

Effective value (from NH_4^+ saturation)	3.95
Theoretical value (from chemical formula)	4.32
Reference value (Barrer and Munday, 1971)	4.37

RESULTS

Characterization of the starting material

The product of zeolitization of perlite consists principally of zeolite Na-P_c. Small amounts of quartz, plagioclase, and biotite (Figure 1) were present in the unreacted starting materials (Christidis *et al.,* 1999). The chemical compositions of the starting material, product, and pure zeolite Na-P_c are given in Table 1. Semi-quantitative analysis by XRD (Brindley, 1980) showed that zeolite Na-P_c is ~80 wt. % of the total material. Based on the XRD analysis, the conversion of volcanic glass to zeolite Na-P_c is virtually complete, although examination of the product by scanning electron microscopy revealed a small number of unreacted glass shards (Christidis *et al.,* 1999).

Compared to the original glass, the chemical composition of the reaction product has less Si and K and more Na (Table 1). Christidis *et al.,* (1999) demonstrated that for these experimental conditions, ~50% of the Si present in the original perlitic glass is released in the liquid phase. Therefore, the observed increase in the amount of accessory minerals relative to the original perlite fines is residual. Based on the parent-glass composition and that of the fluid phase after

https://doi.org/10.1346/CCMN.2000.0480509 Published online by Cambridge University Press

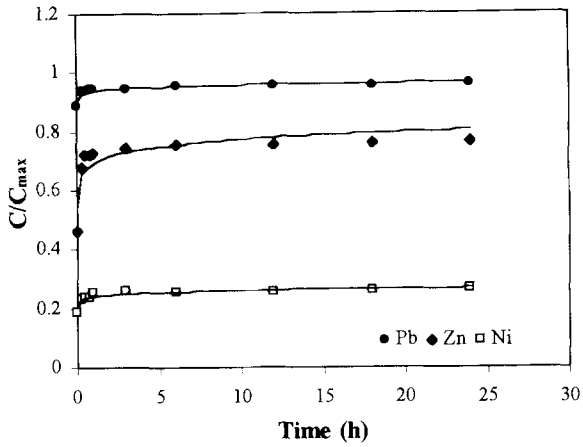

Figure 2. Kinetic curves describing adsorption of Pb, Zn, and Ni by zeolite Na-P_c, where C: the retained metal concentration and C_{max}: the maximum retained metal concentration.

zeolitization (Christidis *et al.*, 1999), the structural formula of pure zeolite Na-P_c was determined (Table 1). The calculated SiO_2:Al_2O_3 and Si:Al ratios of zeolite Na-P_c are 4.45:1 and 2.23:1, respectively, whereas the error value (E%) is within the acceptable limits proposed by Gottardi and Galli (1985).

The CEC of pure zeolite Na-P_c calculated from the structural formula (Table 1) is 4.32 meq g^{-1}, in good agreement with the value reported by Barrer and Munday (1971). In contrast, the CEC of the end product of zeolitization of perlite as determined by NH_4^+ exchange, is 3.16 meq g^{-1} (Table 1). Because the material contains silicate minerals with low exchange capacity, the actual CEC of zeolite Na-P_c determined by NH_4^+ exchange is 3.95 meq g^{-1}, *i.e.*, 10% lower than the value calculated from the structural formula. This difference is attributed to limitations in the quantitative determination of the minerals present by XRD. Exchangeable K, Ca, and Mg balance 19% of the zeolite charge (Table 1). Therefore, before the ion exchange study, the zeolite was rendered homoionic by saturation with 1 M NaCl and subsequent washing until the supernatant liquid was chloride-free.

Cation-exchange study

The kinetic experiments showed that equilibrium is attained rapidly; after 1 h >95% of each metal (C/C_{max}, where C is the retained metal concentration and C_{max} is the maximum retained metal concentration) was retained by zeolite Na-P_c (Figure 2). Therefore, 24 h were allowed for attainment of equilibrium during the construction of the exchange isotherms.

Figure 3 displays the effect of the amount of metal in the solution on adsorption relative to the CEC determined by NH_4^+ exchange. Regardless of the type of metal, the amount adsorbed by zeolite Na-P_c increases steadily and reaches a maximum when its abundance

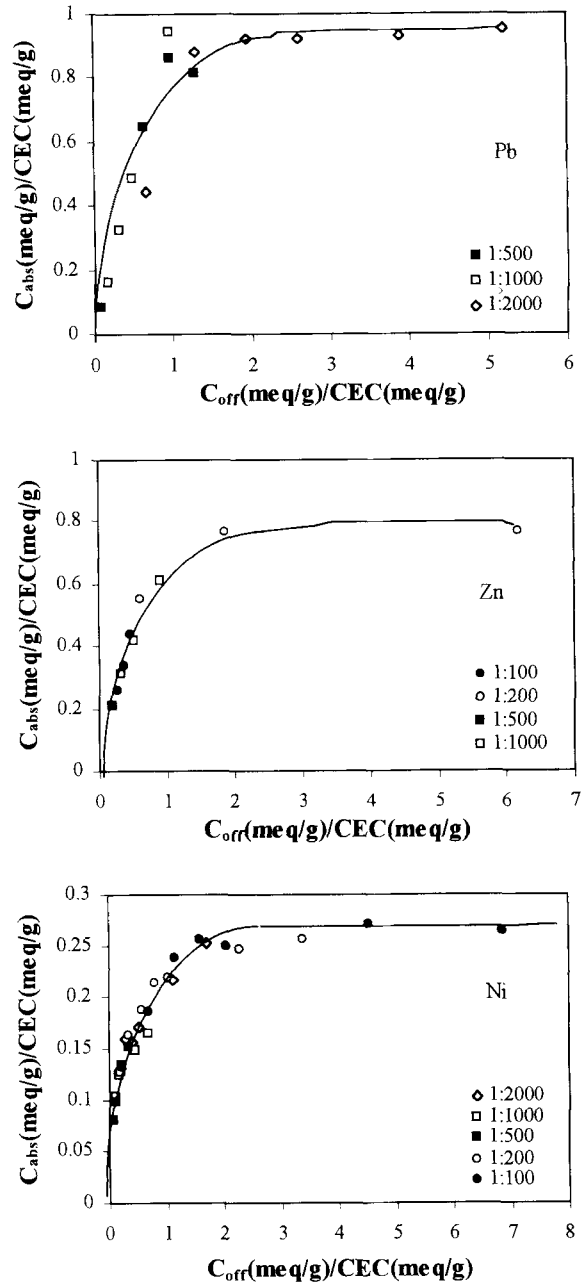

Figure 3. Influence of the amount of metal available, on the absorption of Pb, Zn, and Ni by zeolite Na-P_c, where C_{abs}: the concentration of absorbed metal and C_{off}: the concentration of offered metal.

in solution is twice the CEC. Consequently, the exchange reactions were conducted using initial solutions having cation (M^{2+} + Na^+) concentrations twice the CEC of zeolite Na-P_c as determined by NH_4^+ exchange. Hence, the total normality for Pb was 0.015 N, 0.014 N for Ni, and 0.012 N for Zn. At the end of the experiment, 95% of the theoretically available exchange sites are occupied by Pb. In contrast, Zn oc-

https://doi.org/10.1346/CCMN.2000.0480509 Published online by Cambridge University Press

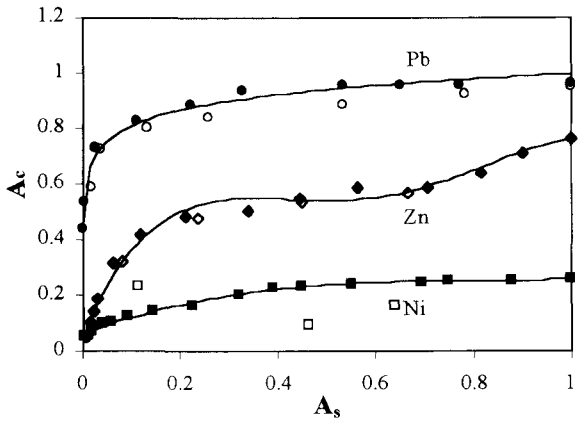

Figure 4. Exchange isotherms for the Na → ½Pb, Na → ½Zn, and Na → ½Ni exchange at 25°C, where A_s and A_c represent the equivalent fractions of the metal in the solution and the zeolite, respectively. The open symbols correspond to the reverse isotherms.

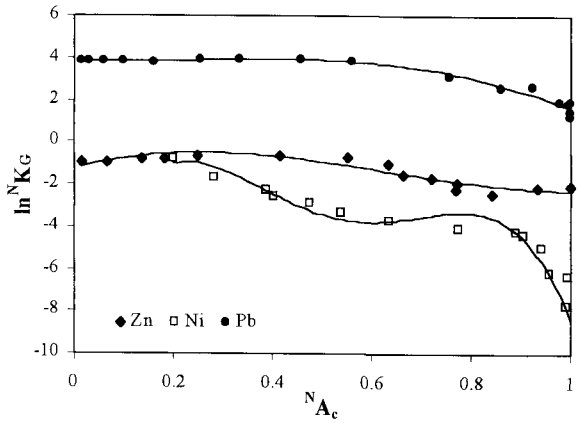

Figure 5. Surface-composition dependance ($^{N}A_c$: normalized equivalent fraction of the metal in the zeolite phase) of the normalized selectivity coefficients ($^{N}K_G$) for Na → ½Pb exchange (●), Na → ½Zn exchange (♦), and Na → ½Ni exchange (□).

cupies 77% and Ni only 27% of the available exchange sites.

The exchange isotherms obtained for the three metals are given in Figure 4. Note that the selectivity of zeolite Na-P_c for the three metals varies between broad limits. The Na → ½Pb exchange isotherm indicates a good selectivity of zeolite Na-P_c for Pb. The selectivity for Pb is sufficient large to consider that the material can remove Pb efficiently from aqueous solutions containing Pb salts, especially at low concentrations. The observed increased selectivity for Pb *vs.* Na is common and is reported in many synthetic and natural zeolites including zeolites X and Y, zeolite A, clinoptilolite, and mordenite (Wiers *et al.,* 1982; Blanchard *et al.,* 1984). The reverse exchange reaction is considerably slower and displays a limited but noticeable hysteresis (Figure 4).

In the Na → ½Zn exchange isotherm, zeolite Na-P_c is relatively selective for Zn at A_s values lower than 0.2. The selectivity for Zn decreases at higher A_s values. The exchange is not complete and is terminated at an A_c value of 0.76, suggesting that not all exchange sites are accessible to Zn. The exchange reaction is fully reversible. The exchange Na → ½Ni is not complete; only 27% of the theoretically available exchange sites are occupied by Ni at the end of the reaction. Reverse experiments were not performed for Ni owing to the small preference of zeolite Na-P_c, yielding to a forward reaction with minimum progress. Prolonged experiments at 15-d equilibrium time did not increase the A_c values for the three metals. As expected for all three metals, the maximum A_c value (Figure 4) is similar to the maximum amount adsorbed during the preliminary experiments (Figure 3).

Figure 5 displays the variation of the normalized-corrected selectivity coefficient $^{N}K_G$ for the three metals, relative to the composition of the zeolite crystals (Kielland plots). The $^{N}K_G$ instead of K_G was used because A_c did not reach unity for any of the three metals. Normalization was performed by multiplying A_c values by the normalization factor $f_N = 1/A_c(max)$, where $A_c(max)$ is the maximum limit of exchange for each metal. The normalized A_c values are denoted $^{N}A_c$. The difference between K_G and $^{N}K_G$ is more important for Zn and Ni compared to Pb, owing to the nearly completed reaction in the latter case.

In the Na → ½Pb exchange, $^{N}K_G$ is nearly constant for A_c values of ≤0.6 and decreases slightly thereafter, indicating that the selectivity for Pb decreases slightly when the exchange sites are progressively filled with this metal. The flat part of the curve corresponds to the steep part of the exchange isotherm (Figure 4) obtained at very low A_s values. A similar trend is shown by Zn, the $^{N}K_G$ values are nearly constant at $^{N}A_c$ values of ≤0.6 and decrease slightly thereafter and finally become constant for $^{N}A_c$ values of ≥0.8. The two Kielland plots are subparallel for $^{N}A_c$ values of <0.8. However, the $^{N}K_G$ values obtained for Zn are considerably lower compared to Pb. The first flat segment corresponds to the steep part of the exchange isotherm, whereas the second flat segment corresponds to A_s values of >0.7 at which A_c also increases (Figure 4). Finally, the $^{N}K_G$ value for Ni decreases as the exchange reaction proceeds. For ln $^{N}K_G$ values of <3, all points plot parallel to the ordinate, *i.e.,* $^{N}A_c$ is nearly constant. As noted above, zeolite Na-P_c is not selective for Ni and the reaction stops (Figures 3 and 4).

The best fits to the Kielland plots for the Na → ½Pb and the Na → ½Zn exchange are shown in Figure 5, whereas the polynomial equations which describe the observed trends better, along with the relative error of the fit (R) values, are listed in Table 2. Attempts to

https://doi.org/10.1346/CCMN.2000.0480509 Published online by Cambridge University Press

Table 2. Best-fit polynomial equations and relative error of the fit (R)[1] which describe the variation of ${}^{N}K_G$ with ${}^{N}A_c$ in the Na → ½Pb and Na → ½Zn exchange.

Exchange	Polynomial equation	Relative error of the fit (R)
Na → ½Pb	$-5.34Pb^3 + 3.48Pb^2 - 0.25Pb + 3.80$	0.128
Na → ½Zn	$39.66Zn^4 - 72.09Zn^3 + 35.85Zn^2 + 4.67Zn - 0.85$	0.135

[1] $R = \sqrt{[\Sigma (\ln {}^{N}K_{G(obs)} - \ln {}^{N}K_{G(calc)})^2]/(N - M - 1)}$.

obtain a polynomial or linear equation for the Kielland plot of the Na → ½Ni exchange resulted in a large R value. The variation of ${}^{N}K_G$ for Pb is best described by a quadratic, and for Zn, by a quartic polynomial equation with low R values (Table 2).

The variations of f_M and f_{Na} (activity coefficients for the cations in the zeolite phase) with respect to ${}^{N}A_c$, where M = Pb or Zn, were calculated according to Gaines and Thomas (1953) and are shown in Figure 6. The f_{Ni} value was not determined owing to the lack of progress of the reaction. As expected, f_M gradually decreases for both metals and f_{Na} increases with increasing metal loading (${}^{N}A_c$).

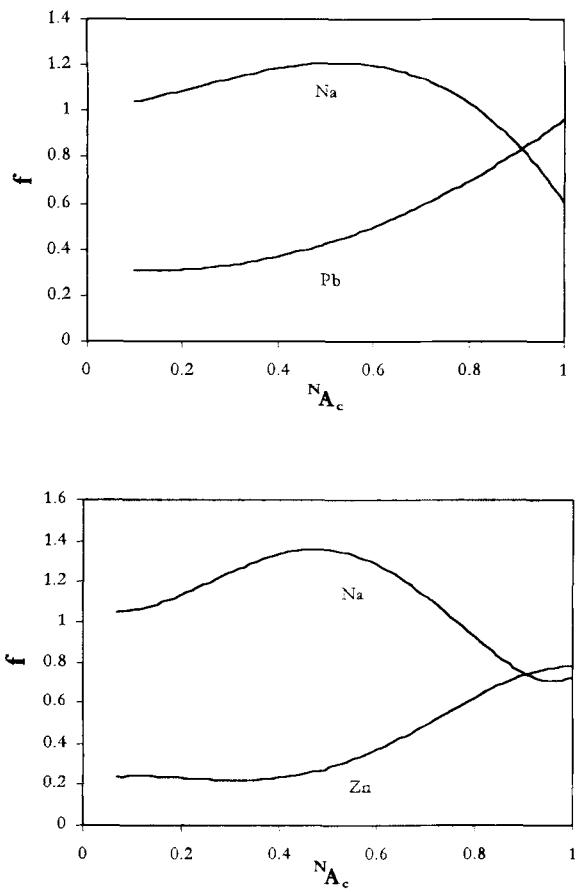

Figure 6. Surface-composition dependance (${}^{N}A_c$: normalized equivalent fraction of the metal in the zeolite phase) of the activity coefficients, f for the vertical axis either being f_M (where M = Pb, Zn) or f_{Na}, during ion exchange.

The polynomial equations used to describe the variation of ${}^{N}K_G$ with ${}^{N}A_c$ were used also to calculate the rational equilibrium constant, K_a, of the Na → ½Pb and the Na → ½Zn exchange reactions, according to Equation (3), except that ${}^{N}K_G$ and ${}^{N}A_c$ are used instead of K_G and A_c. The Gibbs standard free energy of the exchange ($\Delta G°$), calculated according to Equation (4), is given in Table 3. Owing to the low A_c(max) value obtained for the Na → ½Ni exchange (0.27), the f_{Ni} value was large, resulting in a large uncertainty in the calculation of K_a and $\Delta G°$, which were not determined. $\Delta G°$ is negative for Pb and positive for Zn. The results confirm that Pb is selectively preferred by zeolite Na-P_c relative to Zn.

Characterization of the ion-exchange products

The metal for Na exchange affected the structure of zeolite Na-P_c, even for the limited Ni exchange. Exchange of Na by both Zn and Ni decreased the intensity of all diffraction lines (Figure 1). The observed decrease of diffraction intensity and the slight broadening of the 211 and 311 diffraction lines of the Zn form indicate either a decrease of overall crystallinity or a limited collapse of the zeolite Zn-P_c structure and deposition of amorphous material. The broadening of the 211 and 311 peaks was not observed in zeolite Ni-P_c probably owing to limited exchange. Structural transitions to the Na-P_t form frequently reported during exchange (*e.g.*, Barrer and Munday, 1971) were not observed in this study.

Replacement of Na by Pb resulted in collapse of the zeolite structure (Figure 1). The tendency of Pb to absorb X-rays effects the XRD pattern, suggesting the existence of amorphous material, which is not real. However, the contribution of this effect to the observed pattern is not considered significant, because a similar XRD pattern was observed for the back-exchanged zeolite Na-P_c which did not contain a considerable amount of Pb. Therefore, structural collapse is considered irreversible. The broad hump with diffrac-

Table 3. Experimental K_a and $\Delta G°$ values obtained for the Na → ½Pb and the Na → ½Zn exchange in zeolite-P_c.

Exchange	ln K_a	K_a	$\Delta G°$ (KJ eq^{-1})
Na → ½Pb	2.514	12.35	−3.115
Na → ½Zn	−2.208	0.11	2.752

https://doi.org/10.1346/CCMN.2000.0480509 Published online by Cambridge University Press

Table 4. Water loss (wt. %) during the three dehydration stages of zeolite-P_c, according to the type of exchangeable cation. See text for discussion.

Type of zeolite P_c	90–140°C	140–200°C	200–350°C
Na-P_c	61	15.3	23.7
Pb-P_c	45.3	34	20.7
Zn-P_c	41.4	35.6	23

tion maximum at 14 °2θ (Figure 1) either corresponds to the nearly extinguished 110 reflection of zeolite Pb-P_c or suggests the existence of an amorphous or poorly crystalline hydrous phase, possibly Al-rich. Note that the diffraction hump is not present in the XRD trace of the back-exchanged sample (Figure 1). The broad reflections at 22, 28, and 33 °2θ indicate that the decrease of crystallinity during exchange is not associated with complete structural collapse of zeolite P_c. The reflection at 22 °2θ might also indicate deposition of a poorly crystalline silica polymorph, possibly opal-CT. The collapse of the structure of zeolite P_c does not seem to affect the reverse exchange reaction because only limited hysteresis is observed (Figure 4).

The results from the TG-DTG analysis for the Na, Pb, and Zn forms of zeolite-P_c are listed in Table 4. The water loss for the starting material is 17.9%, *i.e.,* 1% more than the value reported by Taylor and Roy (1965). Four percent of the total loss is associated with the abrupt step, which was observed at 80°C (83 ± 4°C; Taylor and Roy, 1965). The DTG curve obtained is similar to gobbinsite (Gottardi and Galli, 1985), except for the lower temperature of the main water-loss event (135 *vs.* 160°C). The main water loss occurs in three steps, a low-temperature event at 90–140°C, an intermediate event at 140–200°C, and a high-temperature event at 200–350°C. At higher temperatures, gradual water loss is observed, which does not exceed 10% of the total loss.

Saturation with Pb modified the hydration characteristics, because Pb-P_c displays lower (13.98%) water loss than Na-P_c. The water loss for Zn-P_c is identical to Na-P_c. The magnitude of the low-temperature event decreases gradually in the order of Na-P_c > Pb-P_c > Zn-P_c, whereas that of the intermediate event is at a minimum in the starting material and similar in Pb and Zn-P_c (Table 4). The occurrence of the high-temperature event is comparable for the three cations. These changes are probably related to some modification of the coordination of H_2O molecules within the zeolite channels. The zeolites Pb-P_c and Zn-P_c have comparable dehydration characteristics, but Zn-P_c has a lower amount of adsorbed water.

The FTIR spectra of the different products are shown in Figure 7. The assignment of the absorption bands follows Breck (1974). Three types of absorption bands are present: a) Bands belonging to the adsorbed

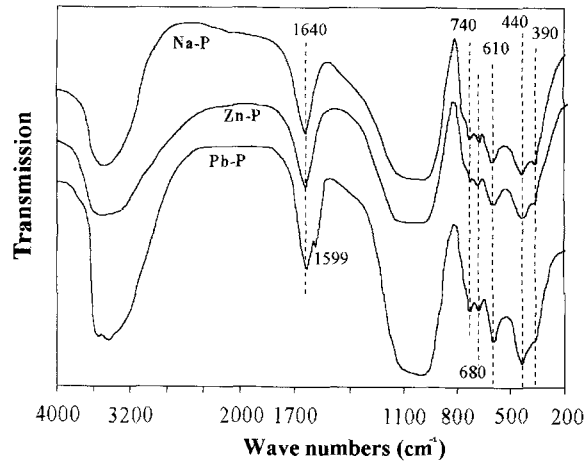

Figure 7. FTIR spectra of zeolite Na-P_c and the solid products of the Na → ½Pb and the Na → ½Zn exchange.

H_2O at 3600, 3440, and 1635 cm^{-1}. The latter is attributed to H-O-H bending; b) Bands which are attributed to the tetrahedral structural units (TO_4, where T = ^{IV}Si or ^{IV}Al. The bands at 1150 and 1000 cm^{-1} are attributed to T-O asymmetric stretching, the bands at 680 and 740 cm^{-1} to T-O symmetric stretching, and the band at 440 cm^{-1} to T-O bending; c) Bands attributed to external linkages (secondary building units). The band at 610 cm^{-1} belongs to double-ring stretching and that at 380 cm^{-1} is attributed to vibrations in pore openings. The small shoulder at 780 cm^{-1} is attributed either to symmetric stretching of external linkages or to the presence of a silica polymorph (probably opal-CT as indicated above) formed by partial dissolution of the zeolite P_c, or both. The lack of absorption bands in the range 3600–3700 cm^{-1}, characteristic of Al-OH-Al stretching, suggests that discrete, poorly crystalline Al-rich phases are not present. Therefore, the broad diffraction hump centered at 13–14 °2θ (Figure 1) probably belongs to zeolite P_c.

The intensity of transmission varies between the different products relative to the starting material. The intensity increases in Pb-P_c and decreases slightly in Zn-P_c. The intensity of the band at 380 cm^{-1} (pore opening) decreases gradually relative to the starting material, being at a minimum in Pb-P_c. The latter is characterized by a well-determined split of the bands, which is attributed to adsorbed H_2O (3600 and 3440 cm^{-1}). A well-defined absorption band occurs at 1599 cm^{-1} (Figure 7) which is attributed to H-O-H bending.

DISCUSSION

The results obtained in this study showed that Pb, and to a lesser degree Zn, replaces Na in zeolite Na-P_c. The Ni for Na exchange is negligible, because only 27% of the available exchange sites are occupied by Ni. The Pauling radii of Zn and Ni are similar (0.74

https://doi.org/10.1346/CCMN.2000.0480509 Published online by Cambridge University Press

and 0.70 Å, respectively) and sufficiently small, so that free diffusion in the channels of zeolite Na-P_c can be assumed. However, the Pauling radius of Pb is significantly greater (1.32 Å), and the radius of the hydrated Zn ion is slightly larger than that of Ni and Pb (4.30, 4.04, and 4.01 Å, respectively; Nightingale, 1959). The dimensions of the zeolite P_c channels (free apperture of 2.8 × 4.9 Å and 3.1 × 4.4 Å; Breck, 1974) suggest that accommodation of all three metals in hydrated form in the channels of the starting material is not possible, without the stripping of H_2O molecules. Therefore, the existence of different ionic radii for the three metals, either anhydrous or hydrated, cannot be invoked as a plausible reason for the different ion-exchange properties observed. Hence, the "molecular-sieving" effect may not be the reason for the lack of progress in the Ni for Na exchange.

Incomplete exchange of Ni for Na was reported for zeolites X and Y by Maes and Cremers (1975) who observed that only 82% of the exchange sites of zeolite X and 68% of Y are occupied by Ni, whereas the Zn for Na exchange is complete (Dyer and Townsend, 1973). Similar observations were made for zeolite 4A (Gal *et al.,* 1971) and for natural Si-rich zeolites such as mordenite (Ni for NH_4^+ exchange; Barrer and Townsend, 1976). The channels of the faujasite-type zeolites are significantly larger than zeolite-P_c and can host six types of exchangeable sites, including type-IV sites (Breck, 1974). Although the different types of exchange sites of zeolite P_c are not known, type-IV sites are not expected for the three cations examined because of their size when fully hydrated. Also type-I sites are not expected to be significant in hydrated zeolites for most divalent cations, whereas type-II and type-III sites are probably most important. Therefore, the observed partial exchange is probably associated with the affinity of the entering cations for the available exchange sites. The observed lack of selectivity for Ni is probably related to its coordination ability and the type of coordination complex it forms in the various channels of zeolite-P_c, similar to synthetic faujasites (Maes and Cremers, 1975). Thus, if Ni preferably enters type-I sites in anhydrous zeolites (*e.g.,* Olson, 1968) it is unlikely to be preferred by the hydrated zeolites. Similar reasoning may account for the incomplete Zn for Na exchange. Zn seems to be more mobile and exhibits a tendency to occupy exchange sites for hydrated cations. The nearly complete Pb for Na exchange suggests that Pb may be selectively preferred in exchange sites with more variable degree of hydration.

The H_2O content of the zeolite Pb-P_c is 22% less than Zn-P_c and Na-P_c, suggesting that an increasing amount of Pb cations are only partially surrounded by H_2O molecules. Also the FTIR spectra (Figure 7) show that absorption bands attributed to vibrations in pore openings are less intense in Pb-P_c compared to Na-P_c and Zn-P_c, *i.e.,* the free space in the zeolite channels is smaller. These changes are probably related to the significant decrease of crystallinity of the zeolite Pb-P_c (Figure 1). In both zeolite Pb-P_c and Zn-P_c, zeolitic water is associated directly with exchangeable cations and/or the zeolite surface, being more tightly bound (inner-sphere complex). This fraction is probably expelled during the high-temperature event. The low-temperature event is believed to be associated with loss of less tightly bound water (outer-sphere complex). This water is expected to be associated with type-III exchange sites. Therefore, we suggest that: a) relative to Zn-P_c, in zeolite Pb-P_c an increasing number of the Pb cations may be located in type-II sites or in those type-III sites forming only an inner-sphere complex with H_2O molecules and b) in Zn-P_c, a greater number of H_2O molecules forms outer-sphere complexes associated both with the Zn cations and the zeolite surface. Thus, the existence of less hydrated Pb ions in the zeolite P_c channels is explained. Although the relative significance of the low-temperature event is greater in zeolite Pb-P_c, the absolute amount of H_2O expelled during that event is significantly greater in zeolite Zn-P_c.

The variation of the normalized selectivity coefficient with increasing loading (Figure 4) suggests a pronounced site homogeneity for ${}^{N}A_c$ values of ≤0.6 with respect to Pb and Zn, but the selectivity for Pb is considerably higher. The similarity of the Kielland plots for Pb and Zn for ${}^{N}A_c$ values of ≤0.8 implies the existence of equivalent exchange sites for the two metals, either type-II or type-III. The two forms have similar dehydration characteristics, in terms of significance of the various dehydration steps (Table 4) and thus support this conclusion. In contrast, Ni is not preferred in these sites. The second plateau in the Kielland plot observed at high Zn loadings, compared to the continuous gradual decrease of ${}^{N}K_G$ for Pb, is attributed to the existence of a number of exchange sites which are occupied by cations associated with a greater number of H_2O molecules (type-III or/and type-II sites with an outer-sphere complex).

The effective removal of Pb, and to a lesser degree Zn, from aqueous solutions by zeolite Na-P_c shown in this study indicates that the material might be used in applications, such as the purification of wastewater from industrial activities (*e.g.,* electroplating) or in the treatment of acid-mine drainage. However, because these industrial effluents usually contain also Fe, Ca, and Mg, which might compete with Pb during ion exchange, the behavior of zeolite Na-P_c must be examined in these systems. The advantages of using zeolite Na-P_c-rich materials in such applications include: a) CEC, which is considerably higher compared to natural zeolite products rich in phillipsite or chabazite and even greater compared to products rich in siliceous zeolites such as mordenite and clinoptilolite and b) fast

retention of large quantities of heavy metals, owing to rapid equilibration during ion exchange. The latter is probably related to the minute size of zeolite Na-P_c crystals (Christidis *et al.,* 1999). Possible disadvantages include: a) modification of the structure during Na $\rightarrow$ ½Pb exchange which may be responsible for the observed slow reverse-exchange reaction and may cause difficulties during regeneration, b) dissolution of zeolite Na-P_c crystals at pH < 2.8, which renders its application difficult in extremely acidic environments such as some acid-mine drainage systems, and c) possible economic constraints regarding zeolite synthesis. Further work is needed to clarify this point, which is beyond the scope of this contribution.

ACKNOWLEDGMENTS

The constructive comments of D.L. Laird and H.S. Sherry improved the text. P.W. Scott corrected the English.

REFERENCES

Aiello, R., Barrer, R.M., and Kerr, I.S. (1971) Molecular sieve zeolites. In *Advances in Chemistry Series, 101,* American Chemical Society, Washington, D.C., 44 pp.

Allison, J.D., Brown, D.S., and Novo-Gradac, K.J. (1991) *MINTEQA2/PRODEFA2, A Geochemical Assessment Model for Environmental Systems, Version 3.0 User's Manual.* U.S. Environmental Protection Agency Report EPA/600/3-91/021, Athens, Georgia, 106 pp.

Antonucci, P.L., Crisafulli, M.L., Giordano, N., and Burriesci, N. (1985) Zeolitization of perlite. *Materials Letters,* **3,** 302–307.

Barrer, R.M. (1982) *Hydrothermal Chemistry of Zeolites.* Academic Press, London, 360 pp.

Barrer, R.M. and Munday, B.M. (1971) Cation exchange reactions of zeolite Na-P. *Journal of the Chemical Society,* **A,** 2909–2914.

Barrer, R.M. and Townsend, R.P. (1976) Transition metal ion exchange Part I. *Journal of the Chemical Society Faraday Transactions I,* **72,** 661–673.

Barrer, R.M., Baynham, J.W., Bultitude, F.W., and Meier, W.M. (1959) Hydrothermal chemistry of the silicates. Part VIII. Low-temperature crystal growth of aluminosilicates, and some gallium and germanium analogues. *Journal of the Chemical Society,* London, 195–208.

Barrer, R.M., Davies, J.A., and Rees, L.V.C. (1968a) Comparison of the ion exchange properties of zeolites X and Y. *Journal of Inorganic and Nuclear Chemistry,* **30,** 2599–2609.

Barrer, R.M., Davies, J.A., and Rees, L.V.C. (1968b) Thermodynamics and thermochemistry of cation exchange in zeolite-Y. *Journal of Inorganic and Nuclear Chemistry,* **30,** 3333–3349.

Barth-Wirsching, U., Höller, H., Klammer, D., and Konrad, B. (1993) Synthetic zeolites formed from expanded perlite: Type, formation conditions and properties. *Mineralogy and Petrology,* **48,** 275–294.

Blanchard, G., Mayunaye, M., and Martin, G. (1984) Removal of heavy metals from waters by means of natural zeolites. *Water Research,* **18,** 1501–1507.

Breck, D.W. (1974) *Zeolite Molecular Sieves.* J. Wiley & Sons, New York, 771 pp.

Breck, D.W. (1983) Synthetic zeolites: Properties and applications. In *Industrial Minerals and Rocks,* S.J. Lefond, ed., Transactions American Institute of Mining, Metallurgical and Petroleum Engineers, 1399–1413.

Brindley, G.W. (1980) Quantitative X-ray mineral analysis of clays. In *Crystal Structures of Clay Minerals and Their X-ray Identification,* G.W. Brindley and G. Brown, eds., Mineralogical Society, London, 411–438.

Burriesci, N., Crisafulli, M.L., Giordano, N., Bart, J.C.J., and Pollizotti, G. (1984) Hydrothermal synthesis of zeolites from low cost natural silica-alumina sources. *Zeolites,* **4,** 384–388.

Christidis, G., Paspaliaris, I., and Kontopoulos, A. (1999) Zeolitization of perlite fines. Part II: Mobilization of chemical elements. *Applied Clay Science,* **15,** 305–324.

Dyer, A. and Townsend, R.P. (1973) The mobility of cations in synthetic zeolites with the faujasite framework-IV. *Journal of Inorganic and Nuclear Chemistry,* **35,** 2993–2999.

Fischer, K. (1963) The crystal structure determination of the zeolite gismondite. $CaAl_2Si_2O_8 \cdot H_2O$. *American Mineralogist,* **48,** 664–672.

Fletcher, P. and Townsend, R.P. (1981) Transition metal ion exchange in zeolites. Part IV. *Journal of the Chemical Society Faraday Transactions II,* **74,** 497–509.

Fletcher, P. and Townsend, R.P. (1982) Transition metal ion exchange in mixed ammonium-sodium X and Y zeolites. *Journal of Chromatography,* **59,** 59–68.

Gaines, G.L. and Thomas, H.C. (1953) Adsorption studies on clay minerals. II. A formulation of the thermodynamics of the exchange adsorption. *Journal of Chemical Physics,* **21,** 714–718.

Gal, I.J., Jancovic, O., Radovanov, P., and Todorovic, M. (1971) Ion exchange equilibria of synthetic 4A zeolite with Ni^{2+}, Co^{2+}, Cd^{2+}, and Zn^{2+} ions. *Journal of the Chemical Society Faraday Transactions I,* **67,** 999–1008.

Giordano, N., Recupero, V., Pino, L., and Bart, J.C.J. (1987) Zeolitization of perlite. A prospective route. *Industrial Minerals,* 83–95.

Gottardi, G. and Galli, E. (1985) *Natural Zeolites.* Springer Verlag, Berlin, 409 pp.

Maes, A. and Cremers, A. (1975) Ion exchange of synthetic zeolites X and Y with Co, Cu and Zn ions. *Journal of the Chemical Society Faraday Transactions I,* **71,** 265–277.

Nawaz, R. and Malone, J.F. (1982) Gobbinsite, a new zeolite mineral from Co. Antrim, North Ireland. *Mineralogical Magazine,* **46,** 365–369.

Olson, D.H. (1968) X-ray evidence for residual water in calcined divalent cation Faujasite-type zeolites. *Journal of Physical Chemistry,* **72,** 1400–1401.

Russell, J.D. (1987) Infrared methods. In *A Handbook of Determinative Methods in Clay Mineralogy,* M.J. Wilson, ed., Blackie, Glasgow, 133–173.

Sherry, H. and Walton, H.F. (1967) The ion exchange properties of zeolites. Part II. Ion exchange in the synthetic zeolite Linde 4A. *Journal of Physical Chemistry,* **71,** 1457–1465.

Taylor, A.M. and Roy, R. (1961) Zeolite studies IV: Na-P zeolites and the ion exchanged derivatives of tetragonal Na-P. *American Mineralogist,* **49,** 656–682.

Wiers, B.H., Grosse, R.J., and Ciliey, W.A. (1982) Divalent and trivalent ion exchange with zeolite-A. *Environmental Science & Technology,* **16,** 617–624.

E-mail address of corresponding author: moirou@metal.ntua.gr

(Received 8 December 1998; accepted 22 May 2000; Ms. 98-137; A.E. Thomas Dombrowski)